Performance Investigation of External Water Cooling for the Fixed Scroll of a Scroll Compressor under Central Tangential Inlet Conditions

Shuai Zhong
School of Chemical Engineering, China University of Mining and Technology, Xuzhou, Jiangsu, China

Abstract: To address the high-temperature hotspot in the central discharge region of the fixed scroll in a scroll compressor, an external water-cooling structure was proposed, in which cooling water enters tangentially through the side annular cavity of the central discharge port and then flows outward through radially divergent channels. A three-dimensional steady-state conjugate heat transfer model was established to investigate the effects of channel number, inlet configuration, and inlet swirl intensity on cooling performance. The results show that, as the number of channels increases from 4 to 12, the average surface temperature of the fixed scroll decreases from 47.219 °C to 45.998 °C, and the maximum surface temperature decreases from 102.730 °C to 99.655 °C, while the pressure drop increases from 4479.72 Pa to 4723.48 Pa. When the number of channels is further increased to 14, both the temperature-related indices and the pressure drop deteriorate. Compared with the double-inlet configuration, the single-inlet configuration achieves lower average and maximum surface temperatures, whereas the double-inlet configuration yields a lower overall average temperature and a lower pressure drop. As the inlet swirl intensity increases, the average surface temperature decreases from 48.954 °C to 46.038 °C, and the maximum surface temperature decreases from 104.22 °C to 99.42 °C, while the pressure drop rises from 1393.08 Pa to 4716.65 Pa. Overall, the 12-channel single-inlet high-swirl configuration is more suitable for enhanced cooling conditions, whereas the 8–10 channel single-inlet medium-swirl configuration provides a better balance between cooling effectiveness and flow resistance.

Keywords: Scroll Compressor; Fixed Scroll Cooling; Radial Flow Channels; Numerical Simulation; Tangential Inlet; External Water Cooling

1. Introduction

Scroll compressors have been widely used in room air conditioners, commercial refrigeration, heat pump systems, and thermal management systems for new energy vehicles because of their compact structure, stable operation, low vibration and noise, and relatively high efficiency [1-3]. Their working principle is based on the orbital motion of the orbiting scroll around the fixed scroll, which forms several crescent-shaped compression chambers between the two scrolls. In this process, low-pressure gas is drawn in from the outer edge, gradually compressed toward the center, and finally discharged as high-pressure gas through the central discharge port [4].

However, during the compression process, the gas is strongly compressed in the central discharge region, generating a large amount of heat and resulting in a pronounced high-temperature hotspot in the central area of the fixed scroll. This region is close to the discharge port, where the thermal load is highly concentrated, and the cooling medium can hardly directly and effectively contact and wash the area because of the limitation of the scroll profile structure [5,6]. Excessive local temperature not only significantly reduces the isentropic efficiency and volumetric efficiency of the compressor, but may also cause thermal deformation of the fixed scroll, changes in axial and radial clearances, deterioration of sealing performance, degradation of lubricating oil, and shutdown due to overheat protection, thereby seriously affecting the long-term reliability and energy performance of the equipment [7,8]. Many studies have shown that high discharge temperature and local overheating are among the main technical

bottlenecks restricting the efficient and stable operation of scroll compressors under high-load or variable operating conditions [9, 10].

Traditional cooling methods, such as natural convection, air cooling, or simple shell cooling, are difficult to meet the heat dissipation requirement of the central region of the fixed scroll under high thermal load conditions [11]. In recent years, external water-cooling technology has attracted increasing attention because of its high heat transfer coefficient and strong cooling directivity. However, existing studies have mainly focused on annular or spiral channel structures. For example, Cai et al. [12] proposed a water-cooled scroll structure and employed the response surface method and a genetic algorithm for multi-objective optimization, which significantly reduced the discharge temperature. However, they did not systematically compare the effects of key parameters such as channel number, inlet configuration, and inlet swirl intensity on cooling performance. Song Shuo et al. [13] analyzed the effects of clearance leakage on the flow and performance of a miniature scroll refrigeration compressor, and Liu Xing Wang et al. [14] studied the axial balance and thermal stress of the orbiting scroll in an electric scroll compressor. However, none of these studies involved the optimal design of external water-cooling channels. In addition, most existing CFD simulations have focused on the internal flow and leakage characteristics of scroll compressors [15,16], and studies on inlet swirl have mainly been carried out for multistage axial-flow or centrifugal compressors [17,18]. Systematic parametric analysis is still lacking for the external radially divergent water-cooling structure targeting the central high-temperature region on the outer side of the fixed scroll [19,20].

Existing studies have mainly focused on annular channels, spiral channels, or internal flow analysis. In contrast, considering the constraint that axial direct water inlet is not feasible because of the central discharge structure, this paper proposes a new cooling structure combining tangential side inlet, annular cavity swirl distribution, and radially divergent channels. In this design, tangential water inlet generates swirl within the annular cavity, promotes circumferentially uniform distribution of the coolant, and enhances the convective heat transfer to the central high-temperature region through radial channels [21,22]. On this basis, systematic comparisons are conducted from three aspects, namely channel number, inlet configuration, and swirl intensity, to reveal the flow and heat transfer characteristics of this type of structure.

2. Physical Models and Numerical Methods

2.1 Governing Equations

This study focuses on the flow and heat transfer process in the external water-cooling structure of the fixed scroll. The cooling medium is liquid water. The fluid domain is solved using the three-dimensional incompressible Navier–Stokes equations and the energy equation, and the buoyancy effect induced by gravity is taken into account in the calculation. Since tangential swirl, radial turning, and near-wall heat transfer coexist in the annular cavity, and local flow separation and reattachment may also occur, the SST k–ω turbulence model is adopted in this study to ensure both near-wall calculation accuracy and the prediction capability for complex flows [23,24].

During the solution process, the continuity equation, momentum equations, and energy equation are solved simultaneously to describe the flow and heat transfer behavior of the coolant in the annular cavity and radial channels. The solid domain is described by the steady-state Fourier heat conduction equation to reflect the temperature distribution characteristics of the fixed scroll under thermal load. The fluid–solid interface is treated using conjugate heat transfer conditions, thereby ensuring the continuity of temperature and heat flux density at the interface. In this way, the distributions of both the coolant flow field and the fixed-scroll temperature field can be obtained simultaneously, providing a basis for the subsequent comparison of cooling performance under different structural parameters.

Continuity equation:

$$\frac{\partial \rho}{\partial t}+\frac{\partial(\rho u)}{\partial x}+\frac{\partial(\rho v)}{\partial y}+\frac{\partial(\rho w)}{\partial z}=0 \quad (1)$$

Among them:

ρ — density, kg/m³;

t — time, s;

u — x-component of the velocity vector, m/s;

v — y-component of the velocity vector, m/s;
w — z-component of the velocity vector, m/s;
In this text, the fluid is liquid water, with a constant density of ρ = 1000 kg/m³.
Energy equation:

$$\frac{\partial(\rho T)}{\partial t}+\frac{\partial(\rho uT)}{\partial x}+\frac{\partial(\rho vT)}{\partial y}+\frac{\partial(\rho wT)}{\partial z}=\frac{\partial}{\partial x}\left(\frac{k}{c_p}\frac{\partial T}{\partial x}\right)+\frac{\partial}{\partial y}\left(\frac{k}{c_p}\frac{\partial T}{\partial y}\right)+\frac{\partial}{\partial z}\left(\frac{k}{c_p}\frac{\partial T}{\partial z}\right)+S_T \quad (2)$$

Among them:
k — fluid heat transfer coefficient, W/(m·K);
cp — specific heat capacity, J/(kg·K);
ST — viscous dissipation term of the fluid, kg/(m·s³)
Momentum equation:

$$\frac{\partial(\rho u)}{\partial t}+div(\rho uu)=\frac{\partial p}{\partial x}+\frac{\partial \tau_{xx}}{\partial x}+\frac{\partial \tau_{yx}}{\partial xy}+\frac{\partial \tau_{zx}}{\partial z}+F_x \quad (3)$$

$$\frac{\partial(\rho u)}{\partial t}+div(\rho uu)=\frac{\partial p}{\partial y}+\frac{\partial \tau_{xy}}{\partial x}+\frac{\partial \tau_{yy}}{\partial xy}+\frac{\partial \tau_{zy}}{\partial z}+F_y \quad (4)$$

$$\frac{\partial(\rho u)}{\partial t}+div(\rho uu)=\frac{\partial p}{\partial z}+\frac{\partial \tau_{xz}}{\partial x}+\frac{\partial \tau_{xz}}{\partial xy}+\frac{\partial \tau_{zz}}{\partial z}+F_z \quad (5)$$

Where:
P — Pressure on the fluid element, Pa;
τ — Component of the viscous force on the element's surface, Pa;
F — External force on the element, N;
u — Velocity vector, m/s;

2.2 Geometric Model

This study focuses on the external water-cooling structure of the fixed scroll in a scroll compressor. The effects of different cooling channel parameters on the temperature distribution on the outer surface of the fixed scroll are mainly analyzed, and their influence on suppressing the high-temperature hotspot in the central discharge region is also investigated. Considering that a discharge structure is located at the center of the fixed scroll, the coolant cannot directly enter vertically from the center. Therefore, a structural configuration combining tangential inlet through the side annular cavity of the central discharge port with radially divergent channels is proposed in this study. The coolant enters tangentially from the side of the annular cavity and forms a circumferential swirl of a certain intensity in the central annular cavity. It then flows outward from the center through multiple radial channels, thereby enhancing the heat transfer capacity on the outer surface of the fixed scroll and improving the temperature distribution. The geometric model is shown in Figure. 1

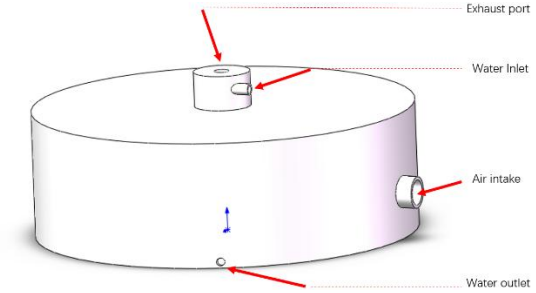

Figure 1. Three-Dimensional Model of the External Water-Cooling Structure

To compare the effects of different structural parameters on cooling performance, six models with 4, 6, 8, 10, 12, and 14 channels were established, respectively. Based on the 12-channel model, further cases with single inlet, double inlet, and three swirl intensities, namely low, medium, and high, were considered. Except for the above variables, all other geometric parameters were kept unchanged, and the main parameters are listed in Table 1. The computational domain includes the solid domain of the fixed scroll and the fluid domain of the cooling water, which were solved simultaneously using the conjugate heat transfer method. The material of the fixed-scroll solid domain was selected as aluminum alloy, and the cooling medium was water. A three-dimensional parametric solid model was established for the geometric model. The analysis mainly focuses on the temperature distribution on the outer surface of the fixed scroll and the heat transfer characteristics under the thermal load in the central discharge region.

Table 1. Main Geometric Parameters

Item	Parameter	Value
Discharge column	Inlet diameter	5 mm
	Inner diameter of annular cavity	16 mm
	Outer diameter of annular cavity	30 mm
Channel structure	Fin height	20 mm
	Fin width	3.8 mm
Fixed scroll outer surface	Diameter	220 mm
Outlet	Diameter	5 mm

2.3 Mesh Generation and Independence Verification

A hybrid meshing strategy was adopted for the computational domain. The solid domain was mainly discretized with tetrahedral meshes. In the fluid domain, local mesh refinement was

applied at the wall boundary layer, the central annular cavity, the inlet and turning regions of the radial channels, and the near-wall regions to capture the swirl boundary layer, temperature gradient, and gravity-induced secondary flow more accurately. To reduce the influence of mesh number on the calculation results, a grid independence test was carried out in this study. Taking the 12-channel high-swirl-intensity model as an example, the average temperature of the fixed scroll and the average outlet velocity in the fluid domain were monitored under different mesh densities. As shown in Figure. 2, when the number of mesh cells exceeded 200,000, the relative variations in the key physical quantities were all less than 0.8%, indicating that the calculation results had basically reached a grid-independent state. Therefore, a mesh scheme with about 400,000 cells was adopted in the subsequent calculations to balance calculation accuracy and computational cost.

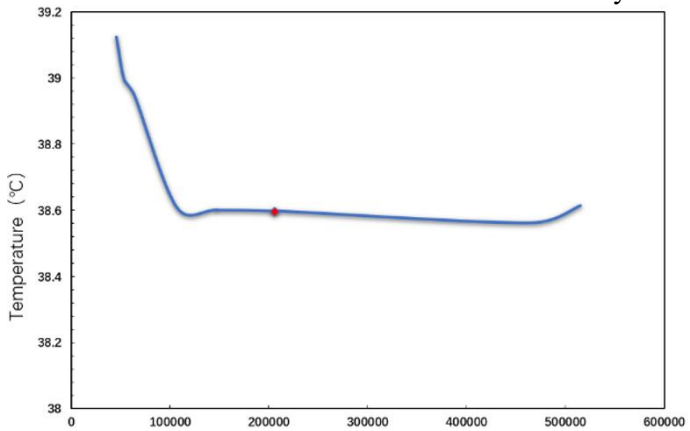

(a) Solid Domain

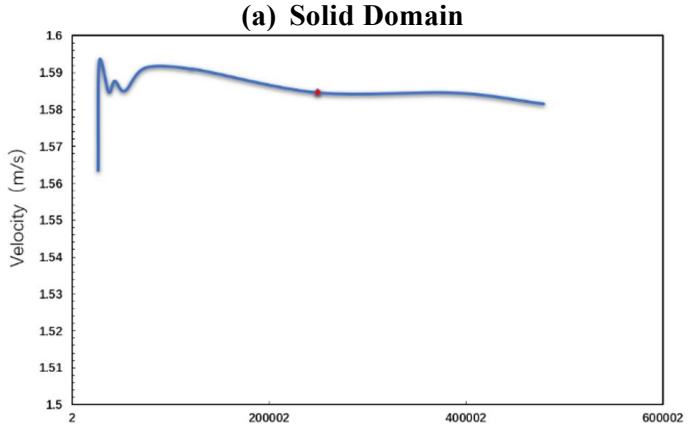

(b) Fluid Domain

Figure 2. Mesh Independence Verification Results

2.4 Boundary Conditions and Solution Settings

Water was used as the cooling medium. The inlet was set as a velocity inlet, and the outlet was set as a pressure outlet. To analyze the effects of different swirl intensities on the flow and heat transfer characteristics, three swirl conditions, namely low, medium, and high, were constructed by varying the inlet velocity profile and vorticity distribution under the same inlet diameter and average inlet velocity. A linear temperature load was applied to the inner surface of the fixed scroll, and a constant-temperature boundary was imposed on the wall of the discharge chamber to represent the thermal boundary characteristic that gradually decays from the central discharge region toward the outer edge. The fluid–solid interface was treated using conjugate heat transfer conditions, and the fluid-side wall satisfied the no-slip condition. Gravity was taken into account in the calculation, and the Boussinesq approximation was adopted to describe the buoyancy effect. The cooling water was regarded as an incompressible Newtonian fluid, and the overall calculation condition was steady state. The SIMPLEC pressure–velocity coupling algorithm was adopted for the numerical solution, and the momentum and energy equations were both discretized using the

second-order upwind scheme. To ensure the reliability of the calculation results, in addition to monitoring the residual convergence, the maximum surface temperature of the fixed scroll and the pressure drop between the inlet and outlet were also monitored. When all monitored quantities became stable during successive iterations, the calculation was considered to have converged. The specific boundary conditions and solution parameters are listed in Table 2.

The linear temperature load on the inner surface of the fixed scroll is given by Eq. (6):

$$T = 20 + 98.8 \times (1 - \frac{x}{76}) \quad (6)$$

where x is the radial distance from the center to the outer edge (unit: mm).

It should be noted that the linear temperature boundary is an engineering simplification intended to represent the dominant temperature gradient of the fixed scroll, rather than to fully reproduce the actual complex temperature field. In the absence of complete experimental temperature measurements or detailed flow-field inversion results, this approach can provide a reasonable thermal boundary condition for analyzing the thermal response of the fixed scroll. The study by Liu Tao et al. [20] also showed that the linear temperature field agrees well with the flow-field-based temperature field in the calculation of thermal deformation and stress.

Table 2. Boundary Conditions and Solution Parameters

Item	Parameter	Value
Water	Temperature	20 °C
	Thermal conductivity	0.6 W/(m·K)
	Specific heat capacity at constant pressure	4182 J/(kg·K)
	Dynamic viscosity	0.001003 kg/(m·s)
Aluminum	Density	2719 kg/m^3
	Specific heat capacity	871 J/(kg·K)
	Thermal conductivity	202.4 W/(m·K)
Inlet boundary	Velocity	2 m/s
Outlet boundary	Gauge pressure	0 Pa
Inner surface of fixed scroll	Linear temperature	(T = 20 + 98.8 *(1 - x/76))

3. Results and Discussion

3.1 Effect of Radial Channel Number on Cooling Performance

Under otherwise identical conditions, six models with 4, 6, 8, 10, 12, and 14 channels were established. Comparative analyses were carried out on the surface temperature distribution, maximum surface temperature, average surface temperature, overall average temperature, and pressure drop of the fixed scroll for each scheme. The results are shown in Figure 3, Figure 4, and Table 3.

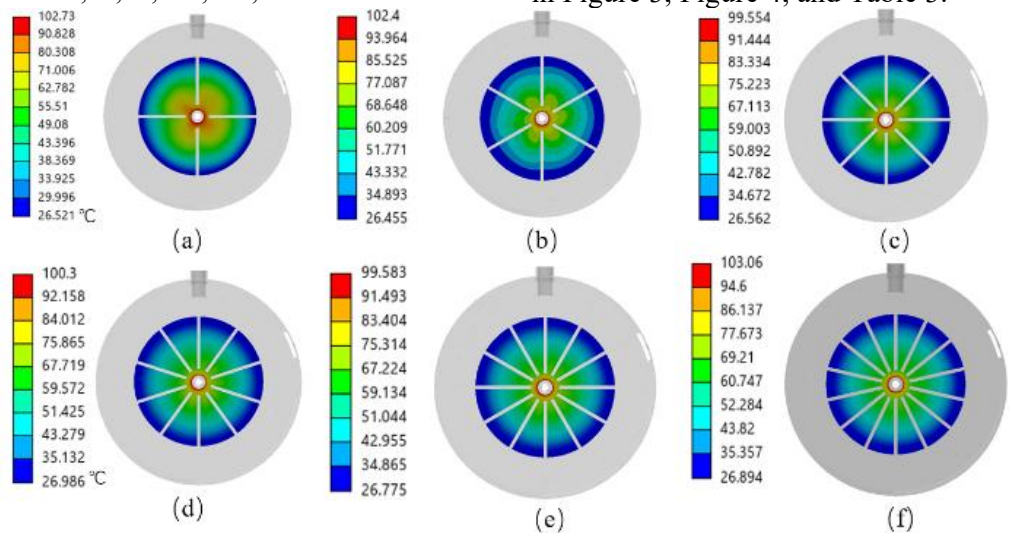

Figure 3. Temperature Distribution on the Outer Surface of the Fixed Scroll under Different Channel Numbers ((a)4-Channel, (b)6- Channel, (c)8- Channel, (d)10- Channel, (e)12- Channel, (f)14- Channel.)

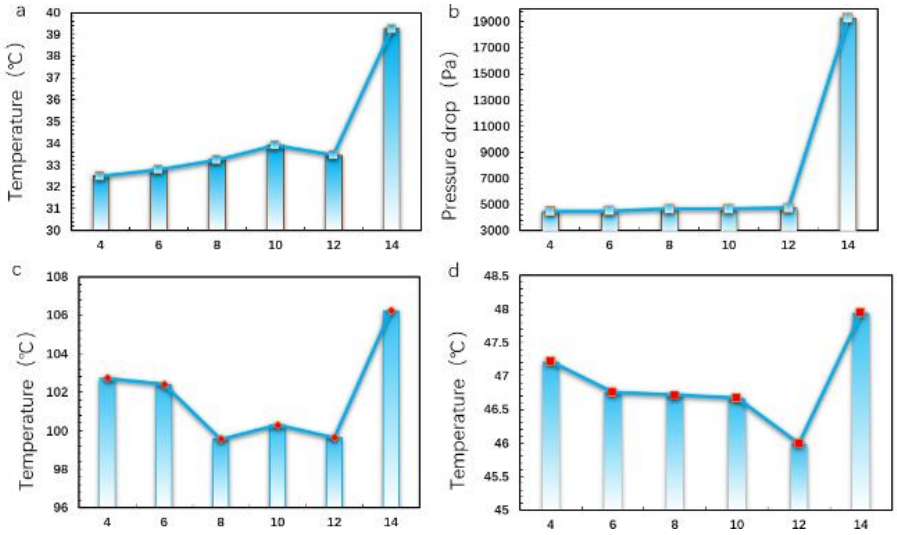

Figure 4. Variation of key Performance Indices with Different Channel Numbers ((a) Overall Average Temperature; (b) Pressure Drop; (c) Maximum Surface Temperature; (d) Surface Average Temperature.)

Table 3. Cooling Performance Parameters under Different Radial Channel Numbers.

Channel number	Minimum surface temperature (°C)	Maximum surface temperature (°C)	Surface average temperature (°C)	Overall average temperature (°C)	Pressure drop (Pa)
4	26.521	102.730	47.219	32.498	4479.72
6	26.455	102.400	46.756	32.785	4528.82
8	26.562	99.554	46.719	33.252	4669.87
10	26.986	100.300	46.676	33.924	4684.37
12	26.775	99.581	45.999	33.451	4737.27
14	26.894	103.061	46.212	33.716	4774.29

It can be observed from the temperature contours in Figure. 3 that an obvious central high-temperature region exists on the surface of the fixed scroll under different channel numbers. This region is close to the discharge port, where the thermal load is concentrated, and the coolant can hardly directly and sufficiently impinge on it because of structural limitations. As the number of radial channels increases, the temperature distribution on the surface of the fixed scroll gradually becomes more uniform. In the 4-channel case, the high-temperature region is relatively large, and the circumferential temperature difference is significant. In the 12-channel case, the petal-shaped high-temperature region is obviously weakened, and the temperature field shows the best uniformity. This indicates that the increase in channel number improves the distribution uniformity of the coolant in the central annular cavity and each radial channel.

Combined with Table 3 and Figure 4, it can be further seen that the average surface temperature of the fixed scroll generally decreases with the increase in channel number. The average surface temperatures of the 4-, 6-, 8-, 10-, and 12-channel schemes are 47.219 °C, 46.756 °C, 46.719 °C, 46.676 °C, and 45.998 °C, respectively. This indicates that, within the range of 4 to 12 channels, the multi-channel structure is indeed beneficial for reducing the overall temperature of the key surface of the fixed scroll. The maximum surface temperature shows a similar trend. Among them, the 8-channel and 12-channel schemes perform better in controlling the central hotspot, and both remain below 100 °C. However, the maximum temperature of the 10-channel scheme rises slightly. This suggests that the local hotspot is related not only to the channel number, but also to the fluid distribution state in the annular cavity and the variation in local flow velocity.

It should be noted that the 14-channel scheme does not further improve the cooling effect. As can be seen from Table 3, when the number of channels reaches 14, the average surface temperature rises to 46.212 °C, the maximum surface temperature increases to 103.06 °C, and the overall average temperature also reaches 33.716 °C. Meanwhile, the pressure drop increases to 4774.29 Pa. It can be found that more channels do not necessarily lead to better performance. When the number of

channels continues to increase, each individual channel becomes narrower, and the flow distribution process between the annular cavity and the channels becomes more complex. As a result, the local loss and friction loss along the flow path increase significantly, which in turn destroys the originally favorable fluid distribution state and finally leads to a deterioration in cooling performance.

From the perspective of the overall average temperature, its variation trend is not completely consistent with that of the average surface temperature. Figure. 4 (a) shows that it first increases and then decreases slightly. The lowest overall average temperature is 32.498 °C for the 4-channel scheme, whereas the highest value is 33.716 °C for the 14-channel scheme. This indicates that the overall average temperature is affected by the area change of the low-temperature region at the periphery. Therefore, it is more suitable for reflecting the overall thermal load level, but it is not appropriate to be used alone to evaluate the cooling performance of the key surface of the fixed scroll. In contrast, the average surface temperature and maximum surface temperature can more directly reflect the cooling effect in the key region on the outer side of the fixed scroll.

Based on Figure. 3, Figure. 4, and Table 3, it can be considered that, within the operating conditions investigated in this study, the preferable channel number lies in the range of 8 to 12. Among them, the 12-channel scheme shows the best performance in terms of average surface temperature, temperature uniformity, and hotspot control. Although its pressure drop is slightly higher, it remains within an acceptable range, and therefore its overall cooling performance is the best. The 8- to 10-channel schemes show a relatively good balance between temperature performance and flow resistance and thus have certain engineering application value.

3.2 Effect of Single Versus Double Inlet on Cooling Performance

Based on the 12-channel structure, the cooling performance of the single-inlet and double-inlet schemes was further compared. The corresponding results are presented in Figure 5 to Figure 7 and Table 4.

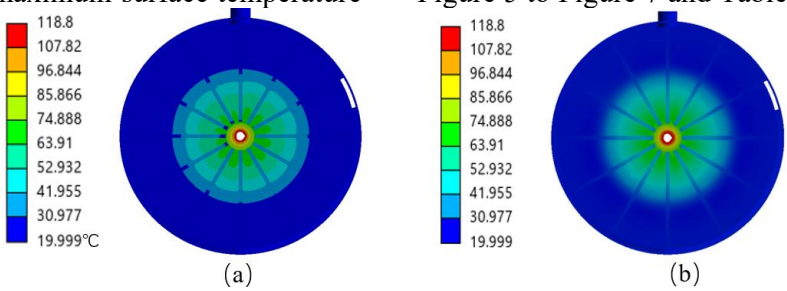

Figure 5. Temperature Distributions for the Single-Inlet (a) and Double-Inlet (b) Schemes.

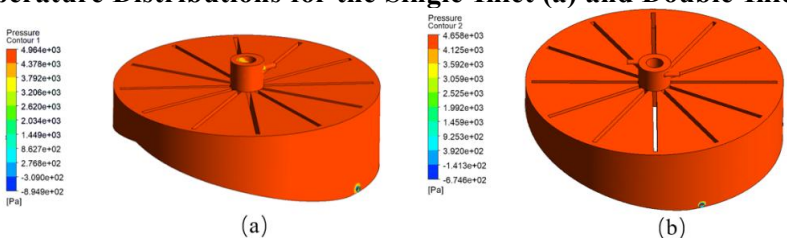

Figure 6. Pressure Distributions in the Fluid Domain for the Single-Inlet((a) and Double-Inlet (b) Schemes.)

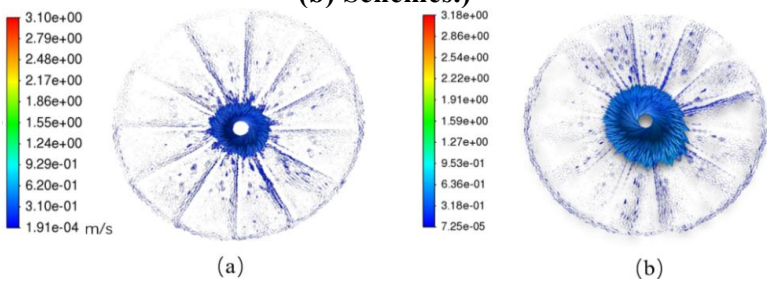

Figure 7. Velocity Vector Distributions in the Fluid Domain for the Single-Inlet (a) and Double-Inlet (b) Schemes.

Table 4. Comparison of main Performance Parameters for the Single-inlet and Double-Inlet Schemes.

Inlet configuration	Minimum surface temperature (°C)	Maximum surface temperature (°C)	Surface average temperature (°C)	Overall average temperature (°C)	Pressure drop (Pa)
12-channel single inlet	26.785	99.65	45.998	33.456	4723.48
12-channel double inlet	26.682	100.19	46.378	32.156	4621.89

It can be seen from Figure 5 that, under both inlet configurations, the surface of the fixed scroll still exhibits the basic distribution characteristic of high temperature in the center and relatively low temperature on the outer side. However, some differences can still be observed in the local temperature field. Under the single-inlet scheme, the high-temperature region is relatively smaller, and the temperature gradient near the center is more concentrated. Under the double-inlet scheme, the temperature distribution is relatively smoother, but the cooling effect in the key high-temperature region is slightly weaker. This phenomenon is consistent with the data listed in Table 4. The average surface temperature and maximum surface temperature of the single-inlet scheme are 45.999 °C and 99.58 °C, respectively, whereas those of the double-inlet scheme are 46.378 °C and 100.19 °C, respectively. In terms of reducing the temperature of the key surface of the fixed scroll and controlling the central hotspot, the single-inlet scheme shows a greater advantage. The variation trend of the overall average temperature is different from that of the surface temperature.

On the other hand, the double-inlet scheme performs better in terms of overall average temperature and pressure drop. As can be seen from Table 4, the overall average temperature of the double-inlet scheme is 32.156 °C, which is lower than the 33.451 °C of the single-inlet scheme. Its pressure drop is 4621.89 Pa, which is also lower than the 4737.27 Pa of the single-inlet scheme. Combined with the variation in the main performance parameters shown in Figure. 8, it can be found that, although the double-inlet scheme is slightly weaker in cooling the key surface, it has a greater advantage in controlling the overall thermal load and flow resistance. The pressure contours of the fluid domain in Figure. 6 also show that the overall pressure distribution of the double-inlet scheme is smoother, whereas the local pressure level of the single-inlet scheme is higher.

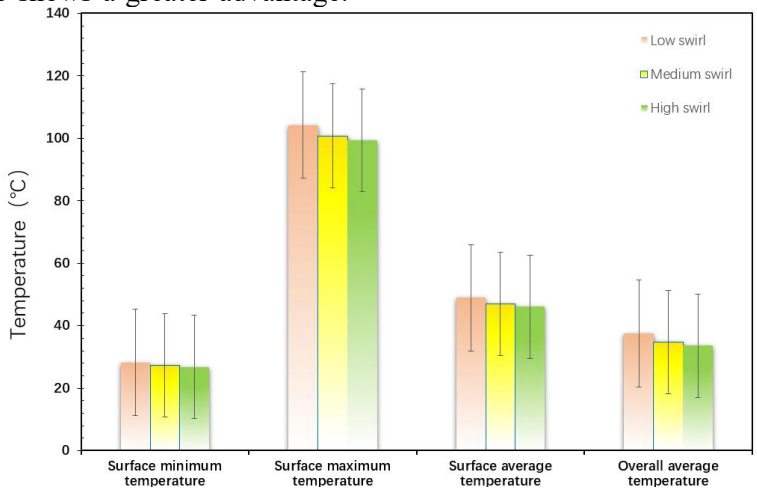

Figure 8. Comparison of Single-Inlet and Double-Inlet Schemes under Different Temperature Indicators.

Figure. 7 further shows that both schemes form a relatively obvious circumferential flow in the central annular cavity. However, in the double-inlet scheme, the fluid distribution becomes more dispersed after entering the annular cavity, and the flow state in each radial channel is also more stable. Therefore, the overall flow resistance is smaller. In contrast, the single-inlet scheme produces a stronger local driving force near the inlet, and the streamlines in some channel directions are more concentrated. This stronger local impingement is beneficial for removing heat near the center, and therefore the average surface temperature and maximum surface temperature are lower.

Based on the above analysis, it can be concluded that the single-inlet and double-inlet schemes have different advantages. The double-inlet scheme is more suitable for operating conditions in which overall thermal load and pressure-drop control are emphasized, whereas the single-inlet scheme is more suitable when the cooling effect on the key surface of the fixed scroll is taken as the main objective. Under the conditions investigated in this study, if priority is given to suppressing the central hotspot and cooling the key surface, the single-inlet scheme is more appropriate. If greater emphasis is placed on overall flow distribution and resistance control, the double-inlet scheme also shows certain advantages.

3.3 Effect of Inlet Swirl Intensity on Cooling Performance

Under the same geometric structure, the cooling performance of three inlet swirl intensity schemes (low, medium, and high) was compared. The results are presented in Figure 9 to Figure 11 and Table 5.

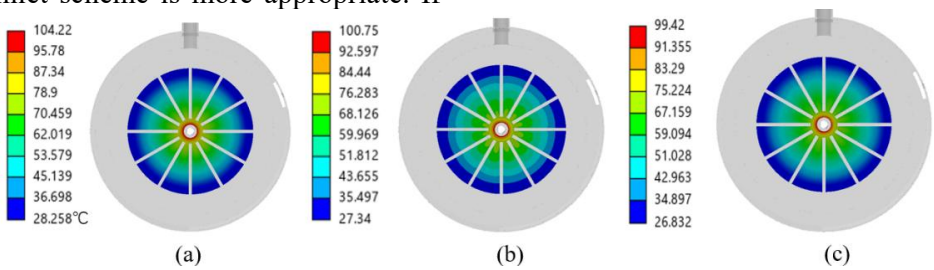

Figure 9. Temperature Distributions on the Fixed Scroll Surface under Low-Swirl (a), Medium-Swirl (b) and High-Swirl(c).

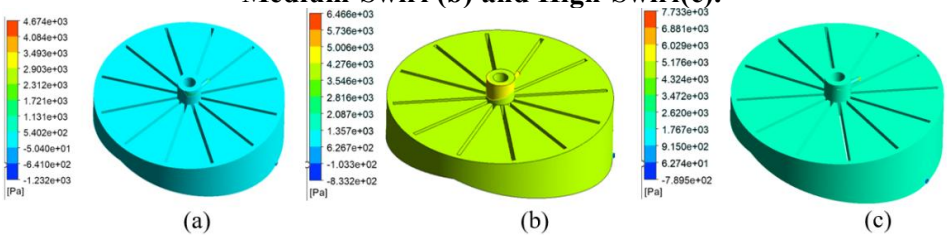

Figure 10. Pressure Distributions in the Fluid Domain under Low-Swirl (a), Medium-Swirl (b) and High-Swirl(c).

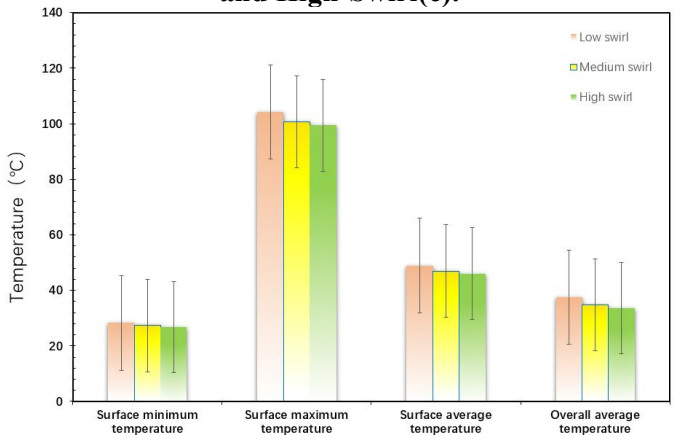

Figure 11. Variation of key Performance Indices under Different Swirl Intensities.

Table 5. Cooling Performance Parameters under Different Inlet Swirl Intensities.

Swirl intensity	Minimum surface temperature (°C)	Maximum surface temperature (°C)	Surface average temperature (°C)	Overall average temperature (°C)	Pressure drop (Pa)
Low	28.258	104.22	48.954	37.515	1393.08
Medium	27.341	100.75	46.940	34.771	3585.48
High	26.832	99.42	46.038	33.563	4716.65

It can be seen from Figure. 9 that, as the inlet swirl intensity increases, the high-temperature region on the surface of the fixed scroll gradually shrinks, and the temperature distribution near the center becomes more uniform. Under the low-swirl condition, a

relatively obvious high-temperature concentration still exists in the central region. Under the medium-swirl condition, the high-temperature region is weakened. Under the high-swirl condition, the central hotspot is controlled most effectively, and the surface temperature field also becomes smoother. The data in Table 5further confirm this trend. Under the low-, medium-, and high-swirl conditions, the average surface temperatures are 48.954 °C, 46.940 °C, and 46.038 °C, respectively, while the maximum surface temperatures are 104.22 °C, 100.75 °C, and 99.42 °C, respectively. In other words, as the inlet swirl intensity increases, the cooling effect on the key surface of the fixed scroll continuously improves.

The overall average temperature shows a similar trend. As indicated in Figure. 11 and Table 5, the overall average temperatures under the low-, medium-, and high-swirl conditions are 37.515 °C, 34.771 °C, and 33.563 °C, respectively. This indicates that increasing the swirl intensity not only improves the local heat transfer in the central region, but also helps reduce the overall thermal load level. This is mainly because stronger swirl can improve the circumferential distribution of the coolant in the annular cavity, allowing the coolant to enter each radial channel more uniformly and thereby enhancing the overall heat transfer capacity.

However, Table 5 also show a very clear trade-off, namely that the pressure drop increases rapidly with increasing swirl intensity. The pressure drops under the low-, medium-, and high-swirl conditions are 1393.08 Pa, 3585.48 Pa, and 4716.65 Pa, respectively. Under the low-swirl condition, the circumferential motion of the fluid is relatively weak, and the distribution effect in the annular cavity is limited. Therefore, the flow loss is the smallest. Under the medium-swirl condition, the circumferential distribution capacity is enhanced, and the pressure drop begins to increase significantly. Under the high-swirl condition, a stronger rotating flow is formed in the annular cavity, and the local loss and friction loss further increase. As a result, the pressure drop reaches the highest value.

The pressure distribution in Figure. 10 also reflects this change. Under the low-swirl condition, the pressure variation in the annular cavity and channels is relatively smooth. Under the medium-swirl condition, more obvious high-pressure regions already appear near the inlet and in the annular cavity. Under the high-swirl condition, the overall pressure level further increases, and the local high-pressure region near the inlet becomes the most prominent. This indicates that, although increasing the swirl intensity can improve the distribution capability of the coolant in the annular cavity and each radial channel, it also significantly increases the flow resistance.

Therefore, from the perspective of temperature control, the high-swirl scheme performs the best. However, if the flow penalty is also taken into account, the medium-swirl scheme has a greater compromise advantage. In other words, the high-swirl scheme is more suitable for design objectives that emphasize enhanced cooling, whereas the medium-swirl scheme is more suitable for practical operating conditions that require a balance between cooling performance and pressure-drop control.

3.4 Comprehensive Comparison and Recommended Optimal Schemes

Table 6 summarizes the main performance indicators under different parameter conditions. Combined with the results presented in the previous sections, it can be seen that the effects of channel number, inlet configuration, and inlet swirl intensity on the external water-cooling performance of the fixed scroll are not completely consistent, and each parameter has its own emphasis.

Table 6. Comprehensive Evaluation of Different Parameter Types.

Parameter type	Scheme	Average surface temperature/°C	Maximum surface temperature/°C	Overall average temperature/°C	Pressure drop/Pa
Channel number	12 channels	45.999	99.58	33.451	4737.27
Channel number	8 channels	46.719	99.554	33.252	4669.87
Inlet configuration	Single inlet	45.999	99.58	33.451	4737.27
Inlet configuration	Double inlet	46.378	100.19	32.156	4621.89
Swirl intensity	High swirl	46.038	99.42	33.563	4716.65
Swirl intensity	Medium swirl	46.941	100.75	34.771	3585.48

From the perspective of channel number, increasing the number of channels is beneficial for reducing the average surface temperature of the fixed scroll and improving temperature uniformity, but it also leads to higher flow resistance. In particular, when the number of channels increases to 14, both the temperature indicators and the pressure drop deteriorate significantly. This indicates that there is an optimal range for channel number, rather than the greater the better. Within the range investigated in this study, the 12-channel scheme shows the best performance in terms of average surface temperature, hotspot control, and overall cooling effect.

From the perspective of inlet configuration, the single-inlet scheme is more likely to generate a stronger local driving force. Therefore, the impingement heat transfer in the key region is more sufficient, resulting in lower average surface temperature and maximum surface temperature. In contrast, the double-inlet scheme produces a smoother flow-field distribution, and therefore yields a lower overall average temperature and a lower pressure drop. Neither scheme is absolutely better than the other. The preferable choice depends on whether the optimization objective places greater emphasis on key surface cooling or on the control of overall thermal load and flow resistance.

From the perspective of swirl intensity, the high-swirl scheme can significantly improve the distribution state in the annular cavity and enhance heat transfer in the central region, and therefore shows the best cooling performance. However, at the same time, the pressure drop also increases more significantly. Although the medium-swirl scheme is slightly weaker than the high-swirl scheme in terms of temperature indicators, it shows a better balance between cooling performance and flow resistance.

Therefore, if enhanced cooling and hotspot control are taken as the main objectives, the combination of 12 channels, single inlet, and high swirl is more suitable. If both cooling performance and flow resistance are considered, the combination of 8–10 channels, single inlet, and medium swirl also shows good engineering application value. This result also indicates that the optimization of the external water-cooling structure of the fixed scroll should not rely only on a single temperature indicator, but should be comprehensively evaluated by combining surface temperature, overall average temperature, and pressure drop. Therefore, within the scope of this study, the combination of 12 channels, single inlet, and high swirl can be recommended for enhanced cooling conditions, whereas the combination of 8–10 channels, single inlet, and medium swirl can be taken as a reference scheme that balances cooling performance and flow resistance.

4. Conclusions

A numerical analysis was conducted on the cooling performance of the external water-cooling structure of the fixed scroll in a scroll compressor, with emphasis on the effects of channel number, inlet configuration, and inlet swirl intensity. The main conclusions are as follows.

(1) There is an optimal range for the number of channels. Within the range of 4 to 12 channels, the average surface temperature decreases and the temperature distribution becomes more uniform as the number of channels increases, but the pressure drop also increases. When the number of channels reaches 14, the performance deteriorates. Among all cases, the 12-channel scheme shows the best overall performance.

(2) The single-inlet scheme is more effective in reducing the average surface temperature and maximum surface temperature of the fixed scroll, whereas the double-inlet scheme is more favorable for reducing the overall average temperature and pressure drop.

(3) Increasing the inlet swirl intensity can significantly enhance heat transfer in the central region and reduce the surface temperature, but it also causes a marked increase in pressure drop. The high-swirl scheme shows the best cooling effect, whereas the medium-swirl scheme provides a better balance.

(4) Based on the overall evaluation, the combination of 12 channels, single inlet, and high swirl is recommended for enhanced cooling. The combination of 8–10 channels, single inlet, and medium swirl is a preferable choice when both cooling performance and flow resistance are taken into account. This study provides a theoretical reference for the optimal design of the external water-cooling structure of the fixed scroll.

References

[1] Zhang Y, Peng B, Zhang P, et al. Key technologies and application of electric scroll compressors: a review. Energies, 2024, 17(7): 1790.

[2] Jiang Z, Harrison D K, Cheng K. Computer-aided design and manufacturing of scroll compressors. Journal of Materials Processing Technology, 2003, 138(1-3): 145-151.

[3] Zheng S, Wei M, Song P, et al. Thermodynamics and flow unsteadiness analysis of trans-critical CO2 in a scroll compressor for mobile heat pump air-conditioning system. Applied Thermal Engineering, 2020, 175: 115368.

[4] Chen Y, Halm N P, Groll E A, et al. Mathematical modeling of scroll compressors—Part I: compression process modeling. International Journal of Refrigeration, 2002, 25(6): 731-750.

[5] Lin C, Chang Y, Liang K, et al. Temperature and thermal deformation analysis on scrolls of scroll compressor. Applied Thermal Engineering, 2005, 25(11-12): 1724-1739.

[6] Hiwata A, Futagami Y, Morimoto T, et al. Deformation control of scroll compressor for CO2 refrigerant. In: International Compressor Engineering Conference at Purdue, 2006.

[7] Wen H, Yan R, Liu L, et al. A review of axial force balance and clearance sealing techniques for energy-efficient scroll compressors. International Journal of Refrigeration, 2025, 176: 298-321.

[8] Chang M S, Park J W, Choi Y M, et al. Reliability evaluation of scroll compressor for system air conditioner. Journal of Mechanical Science and Technology, 2016, 30(10): 4459-4463.

[9] Kwon Y C, Park S J, Ko K W, et al. Correlation on compressor discharge temperature of system A/C applying PWM scroll compressor in cooling mode. Journal of Energy Engineering, 2006, 15(3): 154-159.

[10] Cho H, Chung J T, Kim Y. Influence of liquid refrigerant injection on the performance of an inverter-driven scroll compressor. International Journal of Refrigeration, 2003, 26(1): 87-94.

[11] Kim M H, Bullard C W. Thermal performance analysis of small hermetic refrigeration and air-conditioning compressors. JSME International Journal Series B, 2002, 45(4): 857-864.

[12] Cai Z, Wu Y, Chen H, et al. Design and simulation analysis of water-cooled scroll plate for scroll compressor based on response surface and genetic algorithm. Applied Thermal Engineering, 2025, 269: 125950.

[13] Song S, Zhao Y. Effects of clearance leakage on the flow and performance of a miniature scroll refrigeration compressor. Refrigeration and Air Conditioning, 2023, 37(5): 705-710.

[14] Liu X, Wan C, Kang X. Study on the axial balance of the orbiting scroll in an electric scroll compressor. Fluid Machinery, 2019, 47(11): 13-18.

[15] Cavazzini G, Giacomel F, Benato A, et al. Analysis of the inner fluid-dynamics of scroll compressors and comparison between CFD numerical and modelling approaches. Energies, 2021, 14(4): 1158.

[16] Sun S, Wu K, Guo P, et al. Analysis of the three-dimensional transient flow in a scroll refrigeration compressor. Applied Thermal Engineering, 2017, 127: 1086-1094.

[17] Fang Y, Sun D, Dong X, et al. Effects of inlet swirl distortion on a multi-stage compressor with inlet guide vanes and stall margin enhancement method. Aerospace, 2023, 10(2): 141.

[18] Figurella N, Dehner R, Selamet A, et al. Effect of aerodynamically induced pre-swirl on centrifugal compressor acoustics and performance. SAE International Journal of Passenger Cars - Mechanical Systems, 2015, 8(3): 995-1002.

[19] Sun S, Zhao Y, Li L, et al. Simulation research on scroll refrigeration compressor with external cooling. International Journal of Refrigeration, 2010, 33(5): 897-906.

[20] Sun S, Zhao Y, Li L, et al. Experimental investigation on the scroll refrigeration compressor with external cooling. Proceedings of the Institution of Mechanical Engineers, Part A: Journal of Power and Energy, 2011, 225(6): 832-845.

[21] Darmanis M, Nikas K S, Serbes S A, et al. The effects of inlet conditions on heat transfer in annular swirling decaying flow. In: 10th International Conference from Scientific Computing to Computational

Engineering, 2022.
[22] Abdel-Moneim S A, El-Shamy A R, Berbish N S. Heat transfer to a tangentially injected swirl flow through an artificially roughened annulus. In: 9th International Conference on Aerospace Sciences and Aviation Technology, 2001.
[23] Menter F R. Two-equation eddy-viscosity turbulence models for engineering applications. AIAA Journal, 1994, 32(8): 1598-1605.
[24] Liu T, Wang Y. Thermal stress and deformation analysis of a variable cross-section orbiting scroll based on flow field. Machine Building & Automation, 2015, 44(5): 11-14.

